J. Am. Soc. Mass Spectrom. (2019) 30:1578–1585
DOI: 10.1007/s13361-019-02240-4

RESEARCH ARTICLE

Electron Transfer/Higher Energy Collisional Dissociation of Doubly Charged Peptide Ions: Identification of Labile Protein Phosphorylations

Martin Penkert,[1,2] Anett Hauser,[1,2] Robert Harmel,[1,2] Dorothea Fiedler,[1,2] Christian P. R. Hackenberger,[1,2] Eberhard Krause[1]

[1]Leibniz-Forschungsinstitut für Molekulare Pharmakologie (FMP), Robert-Roessle Str. 10, 13125, Berlin, Germany
[2]Department of Chemistry, Humboldt-Universität zu Berlin, Brook-Taylor-Str. 2, 12489, Berlin, Germany

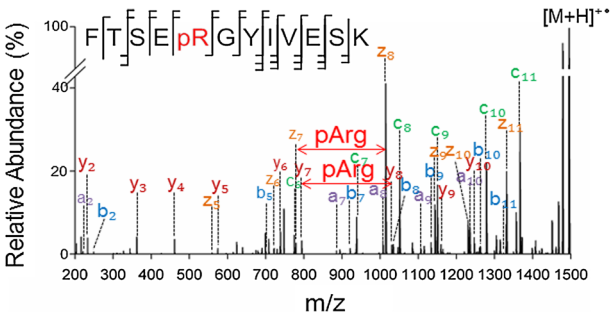

Abstract. In recent years, labile phosphorylation sites on arginine, histidine, cysteine, and lysine as well as pyrophosphorylation of serine and threonine have gained more attention in phosphoproteomic studies. However, the analysis of these delicate posttranslational modifications via tandem mass spectrometry remains a challenge. Common fragmentation techniques such as collision-induced dissociation (CID) and higher energy collisional dissociation (HCD) are limited due to extensive phosphate-related neutral loss. Electron transfer dissociation (ETD) has shown to preserve labile modifications, but is restricted to higher charge states, missing the most prevalent doubly charged peptides. Here, we report the ability of electron transfer/higher energy collisional dissociation (EThcD) to fragment doubly charged phosphorylated peptides without losing the labile modifications. Using synthetic peptides that contain phosphorylated arginine, histidine, cysteine, and lysine as well as pyrophosphorylated serine residues, we evaluated the optimal fragmentation conditions, demonstrating that EThcD is the method of choice for unambiguous assignment of tryptic, labile phosphorylated peptides.

Keywords: Electron transfer/higher energy collisional dissociation, EThcD, Labile phosphorylation, doubly charged peptide ions, Histidine phosphorylation, Lysine phosphorylation, Cysteine phosphorylation, Arginine phosphorylation, Pyrophosphorylation

Received: 22 January 2018/Revised: 7 March 2019/Accepted: 16 March 2019/Published Online: 20 May 2019

Introduction

Beside phosphorylation of serine, threonine, and tyrosine residues, rarely characterized labile phosphorylation sites, for instance phosphorylation of histidine, arginine, and cysteine, have recently been shown to play a crucial role in cell signaling mechanisms [1–5]. The increased interest in identifying and characterizing such alternative phosphorylation events is reflected by the development of site-specific and chemoselective synthetic approaches [6–8], selective enrichment procedures [9–12], and targeted phosphoproteomic strategies [3, 13].

The most prevalent strategy to identify labile phosphorylation sites is based on the bottom-up proteomic approach, which relies on the enzymatic digestion of proteins using trypsin. The generated peptides are analyzed by nanoLC coupled to tandem mass spectrometry (MS/MS). During electrospray ionization (ESI), the majority of tryptic peptides become doubly charged by addition of two protons. These relatively short peptides exhibit a satisfying fragmentation behavior for sequence determination during collision-induced dissociation (CID) or beam-type higher energy collisional dissociation (HCD) [14].

Electronic supplementary material The online version of this article (https://doi.org/10.1007/s13361-019-02240-4) contains supplementary material, which is available to authorized users.

Correspondence to: Martin Penkert; *e-mail:* martin.penkert@gmx.net

Unfortunately, fragmentation of labile phosphopeptides using collision-based fragmentation techniques usually results in pronounced neutral losses, which can hamper unambiguous phosphosite assignment [8, 15]. To cleave the peptide backbone without loss of labile modifications, electron-based fragmentation techniques such as electron capture dissociation (ECD) and electron transfer dissociation (ETD) have been implemented [16–19]. However, fragmentation efficiency during ECD and ETD strongly depends on the charge state of the precursor ions. Both radical-driven techniques perform well for triply and higher charged peptides. Nevertheless, MS/MS spectra of the most frequent doubly charged phosphopeptides, which generally constitute the most important source for phosphosite localization, are dominated by unfragmented, charge-reduced precursor ions, accompanied by insufficient peptide backbone fragmentation [20–22].

Different strategies were pursued to activate the non-dissociative ETD products [23], including elevated gas bath temperatures [20], additional infrared photo-activation (AI-ETD) [24, 25], supplemental low-energy resonant-excitation CID of the electron transfer product population (ETcaD) [26], electron transfer coupled with high-energy resonant-excitation collision-induced dissociation (ET/CID-MS3) [27], and simultaneous electron transfer and collision-induced dissociation [23, 28]. Moreover, derivatization of peptides was performed to enhance the charge density of precursor ions and consequently increase the information content of ETD-MS/MS spectra [29–31]. A fragmentation technique, which combines electron transfer and higher energy collisional dissociation (EThcD), has shown to outperform ETD during fragmentation of doubly charged peptides and enables confident assignment of O-phosphorylations [25, 32, 33]. As a proof of principle, we recently reported that EThcD allows unambiguous assignment of labile cysteine phosphorylation sites and pyrophosphorylated serine and threonine residues [8, 34]. Nevertheless, a broadly applicable, robust tandem mass spectrometric technique, which includes doubly charged precursor ions and, thus, is suitable for phosphoproteomics of labile phosphorylated peptides, covering arginine, histidine, lysine, and cysteine phosphorylation and pyrophosphorylation of serine and threonine, has been lacking. In order to provide such an analytical tool for the proteomic research field, we used our expertise in synthesis of site-specific phosphorylated peptides and validated the performance of EThcD to analyze doubly charged peptides using prevalent search algorithms.

Experimental Section

Synthesis of Phosphopeptides

Peptides were synthesized by Fmoc-based solid-phase peptide synthesis on Tentagel S RAM resin (providing C-terminally amidated sequences) using a Syro II peptide synthesizer (MultiSynTech GmbH). At the desired phosphorylation sites, either the protected phospho-amino acid building block (for pArg peptides) or a precursor (His for pHis, Cys for pCys, azido-Lys for pLys peptides) was incorporated. pHis peptides were obtained upon incubation with potassium phosphoramidate as described by Wei and Matthews [35]. Free pArg peptides were generated by hydrogenation of the bis(2,2,2-trichloroethyl) phosphoramidate previously published by the Seebeck group [36]. As reported by Bertran-Vicente et al., Cys residues were converted to pCys in a three-step synthesis including activation with Ellman's reagent, reaction with light-cleavable phosphite, and deprotection upon UV irradiation [8]. Phospholysine peptides were obtained after reaction of azido-Lys peptides with light-cleavable phosphite and subsequent irradiation yielding the free pLys peptides following the procedure described by the Hackenberger group [7]. Pyrophosphorylated peptides were synthesized following a procedure recently described by Marmelstein et al. [6].

EThcD and HCD Fragmentation Experiments

Phosphopeptides (1 pmol per LC-MS experiment) were analyzed using a reversed-phase capillary liquid chromatography system (Dionex Ultimate 3000 NCS-3500RS Nano, Thermo Scientific, San Jose, CA) coupled to an Orbitrap Fusion mass spectrometer (Thermo Fisher Scientific). Chromatographic separation was performed with an in-house packed 75-µm-inner-diameter PicoTip column (25 cm) packed with ReproSil-Pur C18AQ particles, 3 µm, 120 Å (Dr. Maisch, Germany) at an eluent flow rate of 300 nL min^{-1} using a gradient of 2–50% B in 40 min. Mobile phase A contained 0.1% FA in water, and mobile phase B 0.1% FA in acetonitrile. Ion generation, isolation, and transfer were performed with 2.4-kV spray voltage, 275 °C ion transfer tube temperature and a RF lens voltage of 60%. MS survey scans were acquired at a nominal resolution (R) of 120,000. Only doubly charged precursor ions were subjected to ETD, HCD, and EThcD fragmentation with a dynamic exclusion time of 5 s. MS/MS spectra were acquired with $R = 15{,}000$ at 200 m/z. An automated gain control (AGC) target value of 5e4 and normalized collision energy (NCE) of 35% were chosen for HCD fragmentation. EThcD spectra were measured with AGC target values between 3e4 and 1e5 and a maximum injection time of 1000 ms. Calibrated charge-dependent ETD parameters and ETD reaction times between 75 and 150 ms were used for the ETD process and HCD supplemental activation (sa) was enabled. The sa collision energy varied between 20 and 50% (calculated on m/z and charge state of the precursor ion).

Data Analysis

Data were interpreted with the Proteome Discoverer (Thermo, v. 2.1) and the SEQUEST HT algorithm. The non-fragment filter was used with the following parameters: Precursor ions and charge-reduced precursors were removed within a ± 2 Da and neutral losses within a ± 0.5-Da window. MS/MS spectra were searched against a database containing the synthetic phosphopeptides and common contaminants. Precursor mass tolerance and fragment mass tolerance were set to 10 ppm and 0.02 Da, respectively. Phosphorylation (S, T, Y, C, K, H, and R),

pyrophosphorylation (S and T), and amidation of the C-terminus were searched as variable modifications. The Target Decoy PSM Validator was used to filter peptide spectrum matches (PSMs) with a false discovery rate (FDR) < 0.01. Phosphosite localization was performed with *ptm*RS using diagnostic ions [37]. Three technical replicates of every fragmentation type were merged for data-based analysis. The identification rate (ID rate) was calculated as the quotient of the number of match spectra divided by the number of acquired spectra.

Results and Discussion

To study the fragmentation behavior of doubly charged peptides carrying labile modifications in greater detail, a set of model peptides was synthesized (Table 1). The peptide sequences were based on the amino acid composition of tryptic peptides of identified or putative phosphoproteins [1, 4, 8, 13, 38–40]. Thereby, we incorporated phosphorylations of Cys, His, Arg, and Lys at different positions as well as pyrophosphorylations of serine and threonine.

ETD MS/MS spectra of doubly charged peptides suffered from unreacted and charge-reduced precursor ions, whereas HCD MS/MS spectra exhibited significant peptide backbone fragmentation accompanied with extensive neutral loss of the modification (Figure 1). This observation encouraged us to investigate the influence of supplemental HCD activation after the ETD process. Calibrated charge-dependent ETD parameters with an ETD reaction time of about 100 ms were chosen and the supplemental activation (sa) was varied [41]. Only fragment ion spectra were considered, which did not require the maximum injection time, ensuring that the results were directly related to the applied fragmentation conditions. MS/MS spectra, measured with a sa of 20% NCE, exhibited significant intensities of unreacted precursor ions. An increase of the sa led to its complete fragmentation. Charge-reduced precursor ions represented the base peak in the majority of the spectra (Supplementary Figure S1; Table TS1 and TS2). Neutral losses of 80, 98, and 178 Da from precursor ions were detected with low relative abundances in spectra measured with supplemental activations ranging from 20 to 35% NCE (Supplementary Figure S1). Type and intensity of the neutral loss (NL) varied between modification and peptide sequence (Supplementary Table TS3). Significant in-source fragmentation was not detected.

Table 1. Average Sequest Xcorr Score, Identification Rate, Number of Unique Peptides, and Correct Localized Phosphosites of the Investigated Phosphopeptides at Different Supplemental Activations

Peptide	Peptide sequence (origin)	Average Sequest Xcorr Score per peptide							
		ETD	HCD	EThcD 20%	EThcD 25%	EThcD 30%	EThcD 35%	EThcD 40%	EThcD 50%
ppSer 1	TAVEIDppSDSLK* (ADAP-human)	–	1.98	2.93	3.1	3.6	3.67	3.67	–
ppSer 2	TTAVEIDppSDSLK* (ADAP-human)	–	2.3	3.11	3.34	3.83	3.96	4.1	3.86
ppSer 3	SSEDppSSEEEDKA (Nopp140-mammalian)	–	3.37	3.33	4.14	4.35	4.71	4.94	5
ppThr 4	TTAVEIDppTDSLK* (ADAP-human)	–	2.49	3.1	3.43	3.91	4	4.1	3.82
pHis 1	AVEIDpHDSLK*(ADAP-human)	1.07	2.23	3.71	3.55	4.26	3.82	3.71	–
pHis 2	TAVEIDpHDSLK*(ADAP-human)	1.16	2.77	3.4	3.47	4.41	3.75	3.5	4.16
pHis 3	TTAVEIDpHDSLK* (ADAP-human)	1.21	2.91	2.5	3.14	3.92	3.98	3.9	3.61
pHis 4	FATpHGGYLLQGK (AdhE-*E. coli*)	1.07	3.17	3.22	3.39	4.79	4.91	4.44	4.09
pHis 5	GGRTCpHAAIIAR (PpsA-*E. coli*)	–	3.88	–	2.14	2.84	3.01	3.36	4.05
pCys 1	AVEIDpCDSLK* (ADAP-human)	–	–	3.26	3.8	4.02	–	–	–
pCys 2	TAVEIDpCDSLK* (ADAP-human)	–	2.43	3.16	3.82	3.91	4.16	3.92	3.73
pCys 3	TTAVEIDpCDSLK* (ADAP-human)	1.01	2.71	3.09	4.11	4.24	4.24	4.02	4.03
pCys 4	EQLpCFSLYNAQR* (MgrA-*S. aureus*)	–	3.24	3.1	4	4.04	4.07	3.92	3.74
pCys 5	ENITNLDApCITR* ($IICB^{Glc}$- *E. coli*)	–	3.03	3.44	3.99	4.61	4.18	–	3.56
pArg 1	TAVEIDpRDSLK* (ADAP-human)	0.99	3.31	–	–	4.36	3.9	3.97	–
pArg 2	TTAVEIDpRDSLK* (ADAP-human)	1.26	4.09	–	4.1	4.54	4.12	3.97	–
pArg 3	FTSEpRGYIVESK* (ctsR-*B. subtilis*)	1.46	4.09	3.04	5.07	4.42	5	4.46	5.75
pArg 4	GFLVpREQDPK* (ykoM-*B. subtilis*)	1.11	3.19	–	–	3.62	–	–	–
pArg 5	NGFLVpREQDPK* (ykoM-*B. subtilis*)	1.16	3.05	3.14	4.06	4.16	4.25	4.07	3.89
pLys 1	AVEIDpKDSLK* (ADAP-human)	1.15	2.69	3.36	4.37	4.78	4.74	4.65	4.59
pLys 2	TAVEIDpKDSLK* (ADAP-human)	1.28	3.37	3.39	4.19	4.42	4.49	4.37	3.91
pLys 3	TTAVEIDpKDSLK* (ADAP-human)	1.20	3.41	3.34	4.4	4.79	4.58	4.42	4.26
pLys 4	LpKTEAEMK* (Myoglobin-mammalian)	–	2.97	3.02	3.88	4.18	4.21	4.13	4.17
pLys 5	HLpKTEAEMK* (Myoglobin-mammalian)	1.07	2.51	–	3.94	3.9	3.92	4.01	4
pLys 6	ALELFRpKDAAK* (Myoglobin-mammalian)	1.31	2.63	3.03	–	3.72	–	–	–
	Average Sequest Xcorr score	1.17	3.04	3.20	3.83	4.17	4.16	4.10	4.09
	Identification rate (%)		84.7	35.1	40.0	63.5	55.0	45.3	35.5
	No. of unique peptides	15/25	24/25	20/25	23/25	25/25	22/25	21/25	16/25
	No. of phosphosites with *ptm*RS site probability > 99%	2/25	21/25	17/25	21/25	22/25	21/25	20/25	14/25
	No. of correct assigned phosphosites via *ptm*RS	2/25	13/25	11/25	20/25	21/25	20/25	19/25	13/25

– not identified; *peptide sequence contains an amidated C-terminus

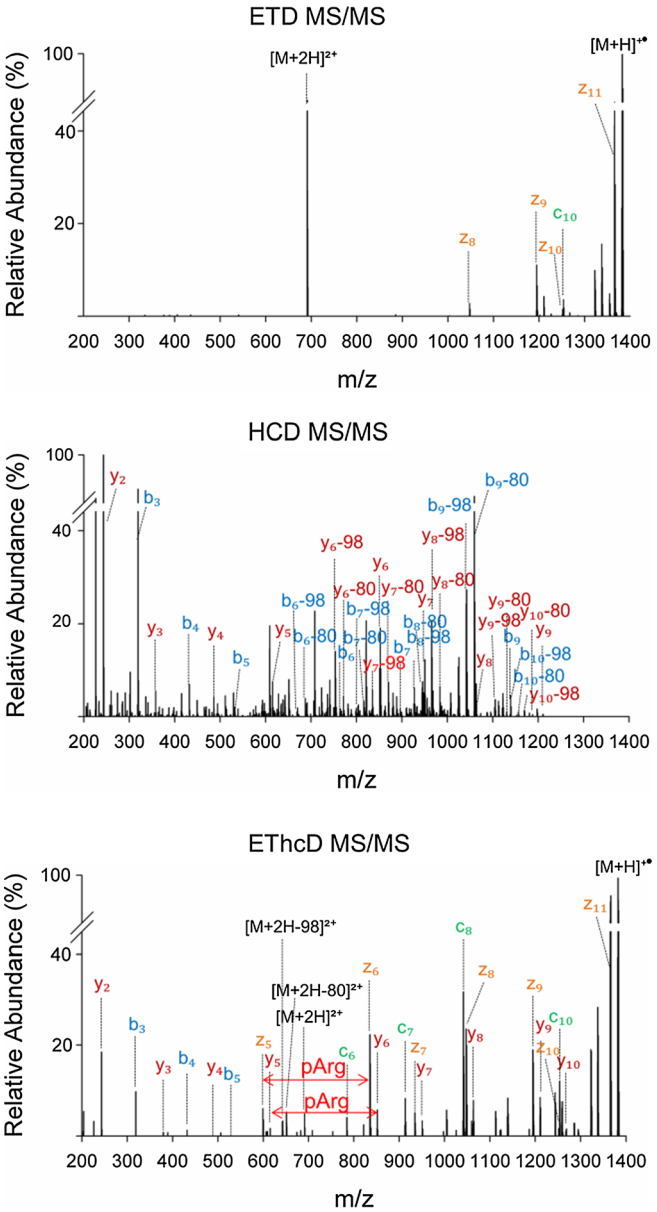

Figure 1. Comparison of ETD, HCD, and EThcD MS/MS spectra of peptide pARG5, showing low peptide backbone fragmentation and sequence coverage during ETD MS/MS. HCD MS/MS generates sufficient precursor fragmentation accompanied with extensive neutral loss of 80 and 98 Da. EThcD MS/MS spectrum provides sufficient sequence coverage without significant neutral loss of the modification

Using a peptide sequence deriving from the adhesion- and degranulation-promoting adapter protein (ADAP) [39], we compared the stability of the different phosphosites by monitoring the relative abundance of fragment ions and neutral losses of those fragments during EThcD and HCD fragmentation. The peptide sequence was phosphorylated at position eight and the amino acid carrying the modification was exchanged (TTAVEIDpXDSLK). In addition, the amino acid sequence contained further potential phospho-acceptors, which allowed observation of potential gas-phase rearrangements [42]. The data impressively illustrated that HCD generates intensive neutral loss of the modification. Due to the lack of fragment ions carrying the phosphate residue, migrations of the moiety could not finally been excluded. In contrast, all investigated labile phosphorylations were stable under EThcD fragmentation conditions, without an indication for phosphate scrambling (Figure 2, Supplementary Figures S2 and S3).

These results encouraged us to calculate the identification rate and monitor the spectral quality and confidence in phosphosite assignment using the search algorithms Sequest and *ptm*RS at different EThcD fragmentation conditions [37]. A supplemental activation of 20% led to the lowest number of unique peptides accompanied with the lowest average Xcorr scores (Table 1 and Figure 4A). Due to the insufficient fragmentation of precursor and charge-reduced precursor ions and the lack of diagnostic fragment ions to pinpoint the modification site, a significant number of false assigned phosphosites were observed. Increasing the secondary HCD activation up to 30% delivered the highest number of unique peptides and correct assigned phosphosites. In addition, the highest Xcorr values were obtained at 30% NCE. This observation is of substantial interest, because similar fragmentation conditions have previously shown to be beneficial for the fragmentation of O-phosphorylated peptides [33]. Consequently, no additional adjustments are required to cover the different phosphorylation types. NCEs of 25 and 35% led either to a slightly reduced number of identified peptides or lower Sequest Xcorr scores and ID rates compared with 30% sa, underlying that EThcD is robust towards small changes in the supplemental activation. Applying a supplemental activation of 40% further enhanced the degree of peptide backbone cleavages (Supplementary Figures S4-S6). Although fragment ions carrying the labile modifications were also increased in its intensities, demonstrating that the different modifications are stable across a broad range of supplemental activations, the Sequest Xcorr score was not significantly improved. In contrast to the results achieved with EThcD, ETD enabled only the correct localization of two phosphorylation sites and provided the lowest Sequest Xcorr score of all examined fragmentation conditions (Table 1). Comparing the EThcD results generated with 30% sa with the prevalent HCD fragmentation technique using a similar AGC target value showed that EThcD had a lower average identification rate, but generates considerably higher average Sequest Xcorr scores. Noteworthy, after EThcD, 22 out of 25 peptides were assigned with a *ptm*RS site probability > 99% and 21 of those matches were correctly localized via the search engine, whereas none of the examined peptides have been identified by ETD without supplemental activation. In addition, two peptides were identified with a *ptm*RS site probability < 99%, exhibiting spectra which allowed unambiguous phosphosite assignment by manual verification (Supplementary Figures S7). In only two cases, the spectral quality was not high enough for correct phosphosite assignment using *ptm*RS. A great challenge was still the confident identification of pHis peptides (Supplementary Table TS5). Beside the lability, an important reason could be the generation of high abundant charge-

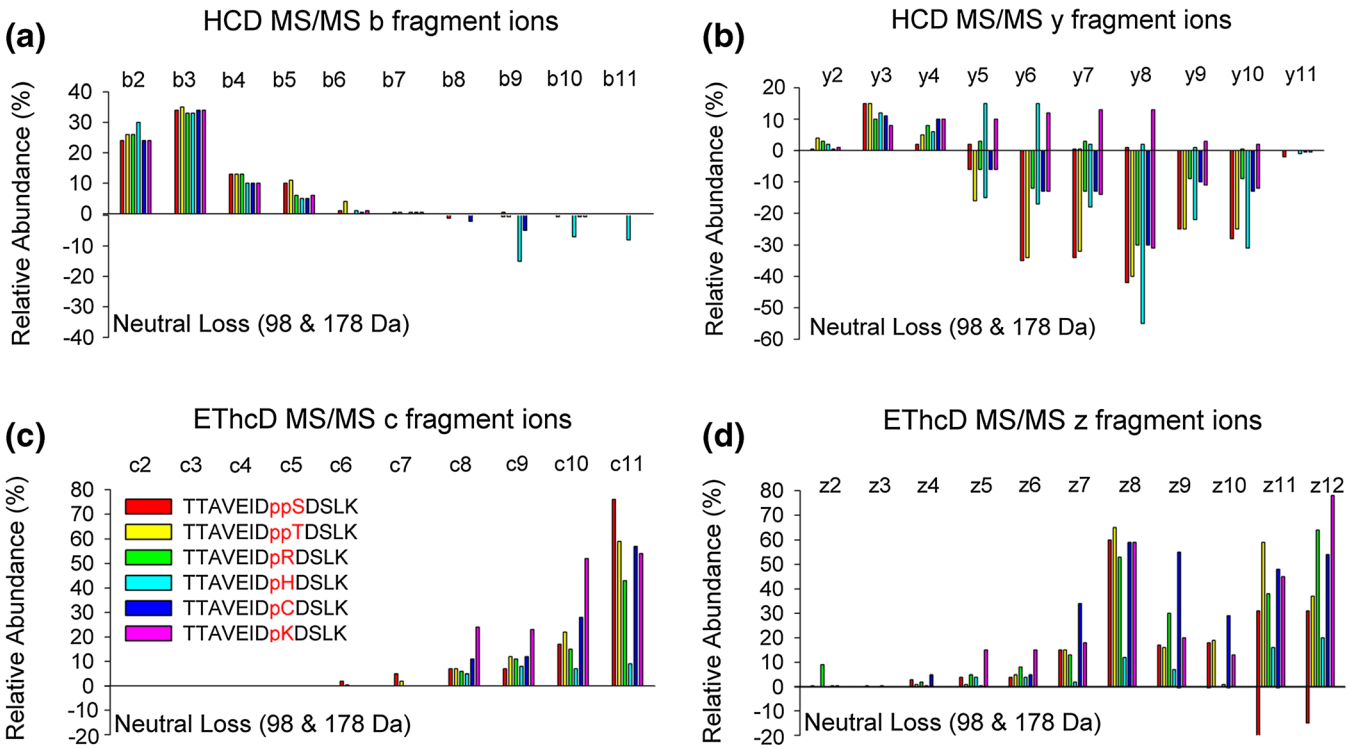

Figure 2. Comparison of the relative abundance of fragment ions and its neutral loss species of peptides ppSer2, ppThr4, pArg2, pHis3, pCys2, pLys3 during HCD (**a**, **b**) and EThcD (**c**, **d**), showing no or tolerable neutral loss during EThcD and extensive neutral loss during HCD fragmentation. Abundances were determined relative to the base peaks of the spectra, which were *m/z* 129.103 and the charge-reduced precursor ion for the HCD and EThcD spectra, respectively

reduced precursor ions accompanied with a low degree of peptide backbone fragmentation. This behavior can also be seen in Figure 2C and D. However, in contrast to EThcD, only 13 phosphosites were correctly assigned using HCD. Especially the identification of pyrophosphorylated peptides, which were misassigned as doubly phosphorylated peptides, constitutes a challenge. But also phosphosite assignment of histidine-, cysteine-, arginine-, and lysine-phosphorylated peptides can be hampered due to extensive neutral loss and the lack of diagnostic fragment ions. Remarkably, the results of the HCD MS/MS spectra show a significant discrepancy between the number of assigned phosphosites with a *ptm*RS site probability > 99% and the number of correct localized phosphosites, further underscoring that the intrinsic lability of the modifications can result in false localized phosphosites during database searches (Table 1 and Supplementary Table TS5). However, collision-based fragmentation techniques can deliver additional information for phosphosite assignment. Previously, phosphohistidine peptides have shown a neutral loss pattern of 80 Da, 98 Da, and 116 Da during ion trap CID [13]. Similar neutral losses were observed with high abundance during HCD. In addition, fragment ion spectra deriving from arginine- and lysine-phosphorylated peptides exhibited the same neutral loss pattern (Supplementary Table TS10), demonstrating that neutral losses of 80 Da, 98 Da, and 116 Da are not unique for phosphohistidine peptides and can give only an indication for a labile phosphorylation.

Besides different neutral loss patterns, phosphoimmonium ions have been used to verify a specific type of phosphorylation [10, 43, 44]. And indeed, two characteristic phosphorylated lysine immonium ions (*m/z* 164.047 and 181.074) were detected for pLys peptides (Figure 3 and Figure S8). Although their abundances are variable and relatively low (Supplementary Table TS11) in combination with high resolved detection, they can function as an indicator to pinpoint a lysine phosphorylation.

Since duty cycle time plays an important role in phosphoproteomic studies, we decided to investigate the

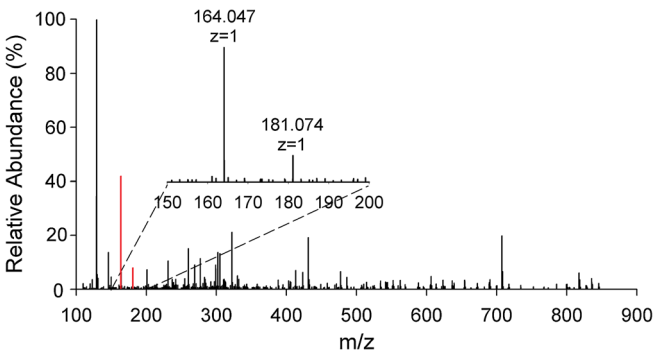

Figure 3. HCD MS/MS spectrum of peptide pLys 4 (LpKTEAEMK) showing two characteristic phosphorylated lysine immonium ions. The diagnostic fragments are highlighted in red

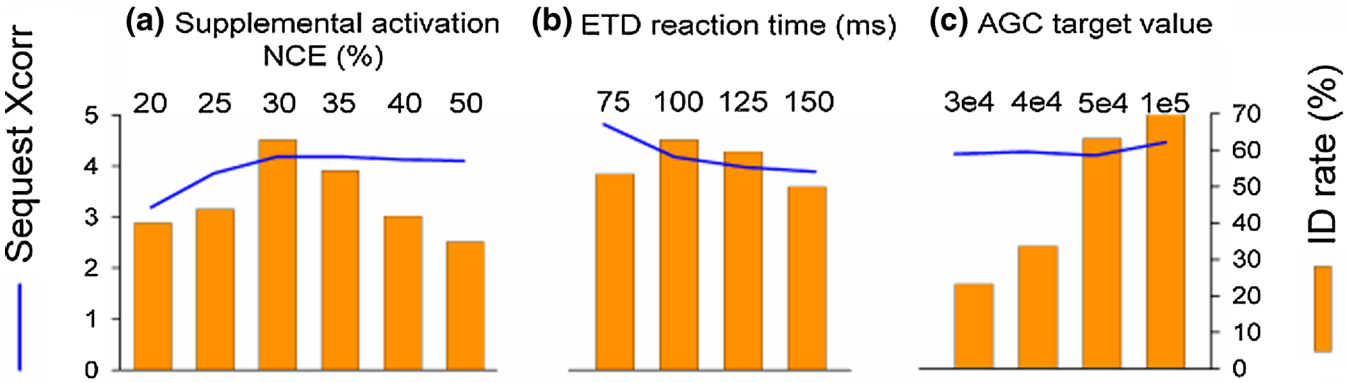

Figure 4. Average Sequest Xcorr score of identified peptides and identification rate depending on EThcD conditions. (**a**) Fixed ETD reaction time (charge-dependent ETD parameters; approx. 100 ms) and different HCD supplemental activation energies. (**b**) EThcD fragmentation with 30% sa and different ETD reaction times. (**c**) EThcD fragmentation with 100 ms reaction time, 30% sa, and different AGC target values

impact of ETD reaction times. Long ETD reaction times shifted the ratio between precursor- and charge-reduced precursor ions towards the non-dissociative ETD product. As a consequence, short reaction times exhibited high abundant precursors, which resulted in increased intensities of b- and y-fragment ions after HCD sa (Supplementary Figure S9). Decreasing the ETD mixing time from 100 ms (charge-dependent ETD parameters) to 75 ms reduced the ID rate and extending also did not significantly improve spectral quality and ID rate (Figure 4B).

According to our observations, EThcD is less sensitive compared with HCD. Decreasing of target values could substantially reduce injection and duty cycle times. However, our data showed that only a minor reduction of the target value to 4e4 already lowered the ID rate (Figure 4C). Doubling of the target value raised the Sequest Xcorr score and ID rate, but did not increase the number of correctly assigned phosphosites (Supplementary Table TS9 and TS12).

To investigate the impact of the concentration in more detail, dilution experiments maxing out the injection time were performed. Depending on the peptide sequence and on the type of modification, lower limits for peptide sequence identification were determined from 0.2 to 38 fmol and 0.4 to 178 fmol for HCD and EThcD, respectively. During HCD, the majority of precursor ions were identified at signal intensities between 1e5 and 2e5 (average signal intensity ≈ 1.6e5) and an average Sequest Xcorr score of 3.09 (Supplementary Table TS13). The lowest signal intensities of identified EThcD spectra were in average about two and a half times higher compared with those of HCD, without a significant drop of the Sequest Xcorr score, 4.25 (Supplementary Table TS14). Remarkably, at this limit of identification, only two phosphosites of the examined 22 peptides were correctly localized using HCD in combination with *ptm*RS, underlying that the higher sensitivity does not provide a great benefit in terms of identification of doubly charged labile phosphorylated peptides. Phosphosite localization via *ptm*RS is done based on diagnostic fragment ions. The lack of those fragments becomes especially noticeable at the limit of peptide sequence identification. A higher number of correctly localized phosphosites were obtained with Sequest (Supplementary Table TS13). In contrast, the majority of labile phosphorylated peptides were correctly assigned at its limit of identification by EThcD. Both Sequest and *ptm*RS provided reliable results and allowed the correct localization of more than 90% of the examined peptides (Supplementary Table TS14).

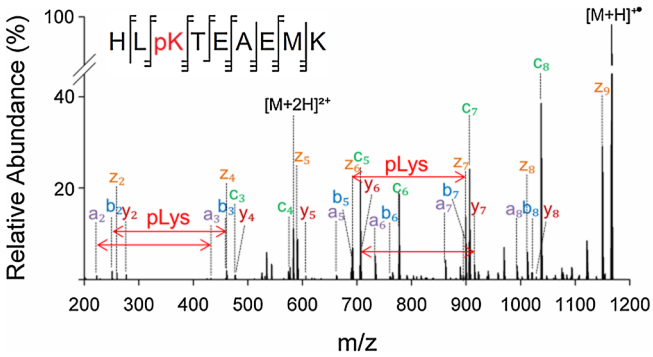

Figure 5. EThcD MS/MS spectrum and cleavage pattern of peptide pLys5, showing fragments from five different ion series, including the diagnostic phosphorylated fragment ions a_3, b_3, c_3, y_7, and z_7

Previously, the observation of b/c- and y/z-ion pairs ("golden pairs") has been reported during EThcD, which increases peptide sequence coverage and facilitates phosphosite assignment [33]. In addition, we detected a- and x-fragment ions. Even though their appearance is less common than those of other fragments, they can be used to validate localized phosphosites. As an example, the EThcD spectrum of peptide pLys 5 is shown in Figure 5, exhibiting a nearly gapless series of a ions, including the diagnostic fragments a_2 and a_3. In combination with fragment ions b_3 and c_3, those fragments form a "golden-triplet," and together with fragments y_7 and z_7, this spectrum exhibits five diagnostic fragment ions for unambiguous phosphosite assignment.

Conclusions

We evaluated the potential of ETD mass spectrometry combined with higher energy collisional dissociation to fragment doubly charged, labile phosphorylated as well as pyrophosphorylated peptides. Our data highlight that labile phosphorylation sites are stable during EThcD. The fragmentation technique allowed unambiguous phosphosite assignment of relatively short, doubly protonated, tryptic peptides, which were not accessible with ETD. Moreover, it improves significantly the confidence in phosphosite assignment compared with HCD. Especially, at the limit of identification, EThcD outperforms HCD, providing more reliable results to identify those delicate modifications. The method delivers phosphosite localization without the need of specific fragmentation conditions, further instrument modifications, and additional peptide derivatization steps, bridging the gap between ETD and HCD. In addition, we show that the appearance of a-and x-ions, and phospholysine immonium ions may provide additional information for reliable localization of labile protein modifications. We envision that EThcD will be the method of choice for verification of putative sites and the identification of new labile protein phosphorylations in vivo by phosphoproteomic approaches.

Supporting Information

Supplemental material, including Supplemental Tables TS1-TS14 and Supplemental Figures S1–S9 are available with this manuscript. The mass spectrometry proteomics data have been deposited to the ProteomeXchange Consortium via the PRIDE [45] partner repository with the dataset identifier PXD012989.

References

1. Trentini, D.B., Suskiewicz, M.J., Heuck, A., Kurzbauer, R., Deszcz, L., Mechtler, K., Clausen, T.: Arginine phosphorylation marks proteins for degradation by a Clp protease. Nature. **539**, 48–53 (2016)
2. Fuhrmann, J., Schmidt, A., Spiess, S., Lehner, A., Turgay, K., Mechtler, K., Charpentier, E., Clausen, T.: McsB is a protein arginine kinase that phosphorylates and inhibits the heat-shock regulator CtsR. Science. **324**, 1323–1327 (2009)
3. Hauser, A., Penkert, M., Hackenberger, C.P.R.: Chemical approaches to investigate labile peptide and protein phosphorylation. Acc. Chem. Res. **50**, 1883–1893 (2017)
4. Sun, F., Ding, Y., Ji, Q.J., Liang, Z.J., Deng, X., Wong, C.C.L., Yi, C.Q., Zhang, L., Xie, S., Alvarez, S., Hicks, L.M., Luo, C., Jiang, H.L., Lan, L.F., He, C.: Protein cysteine phosphorylation of SarA/MgrA family transcriptional regulators mediates bacterial virulence and antibiotic resistance. Proc. Natl. Acad. Sci. U. S. A. **109**, 15461–15466 (2012)
5. Schmidt, A., Trentini, D.B., Spiess, S., Fuhrmann, J., Ammerer, G., Mechtler, K., Clausen, T.: Quantitative phosphoproteomics reveals the role of protein arginine phosphorylation in the bacterial stress response. Mol. Cell. Proteomics. **13**, 537–550 (2014)
6. Marmelstein, A.M., Yates, L.M., Conway, J.H., Fiedler, D.: Chemical pyrophosphorylation of functionally diverse peptides. J. Amer. Chem. Soc. **136**, 108–111 (2014)
7. Bertran-Vicente, J., Serwa, R.A., Schumann, M., Schmieder, P., Krause, E., Hackenberger, C.P.R.: Site-specifically phosphorylated lysine peptides. J. Amer. Chem. Soc. **136**, 13622–13628 (2014)
8. Bertran-Vicente, J., et al.: Chemoselective synthesis and analysis of naturally occurring phosphorylated cysteine peptides. Nat. Commun. **7**, 12073 (2016)
9. Trentini, D.B., Fuhrmann, J., Mechtler, K., Clausen, T.: Chasing phosphoarginine proteins: development of a selective enrichment method using a phosphatase trap. Mol. Cell. Proteomics. **13**, 1953–1964 (2014)
10. Fuhs, S.R., Meisenhelder, J., Aslanian, A., Ma, L., Zagorska, A., Stankova, M., Binnie, A., Al-Obeidi, F., Mauger, J., Lemke, G., Yates 3rd, J.R., Hunter, T.: Monoclonal 1- and 3-phosphohistidine antibodies: new tools to study histidine phosphorylation. Cell. **162**, 198–210 (2015)
11. Conway, J.H., Fiedler, D.: An affinity reagent for the recognition of pyrophosphorylated peptides. Angew. Chem. Int. Edit. Engl. **54**, 3941–3945 (2015)
12. Fuhrmann, J., Subramanian, V., Thompson, P.R.: Synthesis and use of a phosphonate amidine to generate an anti-phosphoarginine-specific antibody. Angew. Chem. Int. Ed. Engl. **54**, 14715–14718 (2015)
13. Oslund, R.C., Kee, J.M., Couvillon, A.D., Bhatia, V.N., Perlman, D.H., Muir, T.W.: A phosphohistidine proteomics strategy based on elucidation of a unique gas-phase phosphopeptide fragmentation mechanism. J. Amer. Chem. Soc. **136**, 12899–12911 (2014)
14. Nagaraj, N., D'Souza, R.C.J., Cox, J., Olsen, J.V., Mann, M.: Feasibility of large-scale phosphoproteomics with higher energy collisional dissociation fragmentation. J. Proteome Res. **9**, 6786–6794 (2010)
15. Potel, C.M., Lemeer, S., Heck, A.J.R.: Phosphopeptide fragmentation and site localization by mass spectrometry; an update. Anal. Chem. **91**, 126–141 (2018)
16. Sarbu, M., Ghiulai, R.M., Zamfir, A.D.: Recent developments and applications of electron transfer dissociation mass spectrometry in proteomics. Amino Acids. **46**, 1625–1634 (2014)
17. Kowalewska, K., Stefanowicz, P., Ruman, T., Fraczyk, T., Rode, W., Szewczuk, Z.: Electron capture dissociation mass spectrometric analysis of lysine-phosphorylated peptides. Biosci. Rep. **30**, 433–443 (2010)
18. Sweet, S.M.M., Bailey, C.M., Cunningham, D.L., Heath, J.K., Cooper, H.J.: Large scale localization of protein phosphorylation by use of electron capture dissociation mass spectrometry. Mol. Cell. Proteomics. **8**, 904–912 (2009)
19. Kim, M.S., Pandey, A.: Electron transfer dissociation mass spectrometry in proteomics. Proteomics. **12**, 530–542 (2012)
20. Pitteri, S.J., Chrisman, P.A., McLuckey, S.A.: Electron-transfer ion/ion reactions of doubly protonated peptides: effect of elevated bath gas temperature. Anal. Chem. **77**, 5662–5669 (2005)
21. Good, D.M., Wirtala, M., McAlister, G.C., Coon, J.J.: Performance characteristics of electron transfer dissociation mass spectrometry. Mol. Cell. Proteomics. **6**, 1942–1951 (2007)
22. Iavarone, A.T., Paech, K., Williams, E.R.: Effects of charge state and cationizing agent on the electron capture dissociation of a peptide. Anal. Chem. **76**, 2231–2238 (2004)
23. Riley, N.M., Coon, J.J.: The role of electron transfer dissociation in modern proteomics. Anal. Chem. **90**, 40–64 (2017)
24. Ledvina, A.R., McAlister, G.C., Gardner, M.W., Smith, S.I., Madsen, J.A., Schwartz, J.C., Stafford Jr., G.C., Syka, J.E., Brodbelt, J.S., Coon, J.J.: Infrared photoactivation reduces peptide folding and hydrogen-atom migration following ETD tandem mass spectrometry. Angew. Chem. Int. Ed. Engl. **48**, 8526–8528 (2009)
25. Riley, N.M., Westphall, M.S., Hebert, A.S., Coon, J.J.: Implementation of activated ion electron transfer dissociation on a quadrupole-Orbitrap-linear ion trap hybrid mass spectrometer. Anal. Chem. **89**, 6358–6366 (2017)
26. Swaney, D.L., McAlister, G.C., Wirtala, M., Schwartz, J.C., Syka, J.E.P., Coon, J.J.: Supplemental activation method for high-efficiency electron-transfer dissociation of doubly protonated peptide precursors. Anal. Chem. **79**, 477–485 (2007)
27. Liu, C.W., Lai, C.C.: Effects of electron-transfer coupled with collision-induced dissociation (ET/CID) on doubly charged peptides and phosphopeptides. J. Amer. Soc. Mass Spectrom. **22**, 57–66 (2011)
28. Campbell, J.L., Hager, J.W., Le Blanc, J.C.: On performing simultaneous electron transfer dissociation and collision-induced dissociation on multiply protonated peptides in a linear ion trap. J. Amer. Soc. Mass Spectrom. **20**, 1672–1683 (2009)
29. Asakawa, D., Osaka, I.: High-confidence sequencing of phosphopeptides by electron transfer dissociation mass spectrometry using dinuclear zinc(II) complex. Anal. Chem. **88**, 12393–12402 (2016)
30. Frey, B.L., Ladror, D.T., Sondalle, S.B., Krusemark, C.J., Jue, A.L., Coon, J.J., Smith, L.M.: Chemical derivatization of peptide carboxyl

groups for highly efficient electron transfer dissociation. J. Amer. Soc. Mass Spectrom. **24**, 1710–1721 (2013)
31. Ko, B.J., Brodbelt, J.S.: Enhanced electron transfer dissociation of peptides modified at C-terminus with fixed charges. J. Amer. Soc. Mass Spectrom. **23**, 1991–2000 (2012)
32. Frese, C.K., Altelaar, A.F.M., van den Toorn, H., Nolting, D., Griep-Raming, J., Heck, A.J.R., Mohammed, S.: Toward full peptide sequence coverage by dual fragmentation combining electron-transfer and higher-energy collision dissociation tandem mass spectrometry. Anal. Chem. **84**, 9668–9673 (2012)
33. Frese, C.K., Zhou, H.J., Taus, T., Altelaar, A.F.M., Mechter, K., Heck, A.J.R., Mohammed, S.: Unambiguous phosphosite localization using electron-transfer/higher-energy collision dissociation (EThcD). J. Proteome Res. **12**, 1520–1525 (2013)
34. Penkert, M., Yates, L.M., Schumann, M., Perlman, D., Fiedler, D., Krause, E.: Unambiguous identification of serine and threonine pyrophosphorylation using neutral-loss-triggered electron-transfer/higher-energy collision dissociation. Anal. Chem. **89**, 3672–3680 (2017)
35. Wei, Y.F., Matthews, H.R.: Identification of phosphohistidine in proteins and purification of protein-histidine kinases. Methods Enzymol. **200**, 388–414 (1991)
36. Hofmann, F.T., Lindemann, C., Salia, H., Adamitzki, P., Karanicolas, J., Seebeck, F.P.: A phosphoarginine containing peptide as an artificial SH2 ligand. Chem. Commun. **47**, 10335–10337 (2011)
37. Taus, T., Kocher, T., Pichler, P., Paschke, C., Schmidt, A., Henrich, C., Mechtler, K.: Universal and confident phosphorylation site localization using phosphoRS. J. Proteome Res. **10**, 5354–5362 (2011)
38. Elsholz, A.K., Turgay, K., Michalik, S., Hessling, B., Gronau, K., Oertel, D., Mader, U., Bernhardt, J., Becher, D., Hecker, M., Gerth, U.: Global impact of protein arginine phosphorylation on the physiology of Bacillus subtilis. Proc. Natl. Acad. Sci. U. S. A. **109**, 7451–7456 (2012)
39. Sylvester, M., Kliche, S., Lange, S., Geithner, S., Klemm, C., Schlosser, A., Grossmann, A., Stelzl, U., Schraven, B., Krause, E., Freund, C.: Adhesion and degranulation promoting adapter protein (ADAP) is a central hub for phosphotyrosine-mediated interactions in T cells. PLoS One. **5**, e11708 (2010)
40. Bhandari, R., Saiardi, A., Ahmadibeni, Y., Snowman, A.M., Resnick, A.C., Kristiansen, T.Z., Molina, H., Pandey, A., Werner, J.K., Juluri, K.R., Xu, Y., Prestwich, G.D., Parang, K., Snyder, S.H.: Protein pyrophosphorylation by inositol pyrophosphates is a posttranslational event. Proc. Natl. Acad. Sci. U. S. A. **104**, 15305–15310 (2007)
41. Rose, C.M., Rush, M.J., Riley, N.M., Merrill, A.E., Kwiecien, N.W., Holden, D.D., Mullen, C., Westphall, M.S., Coon, J.J.: A calibration routine for efficient ETD in large-scale proteomics. J. Amer. Soc. Mass Spectrom. **26**, 1848–1857 (2015)
42. Bertran-Vicente, J., Schuemann, M., Hackenberger, C.P.R., Krause, E.: Gas-phase rearrangement in lysine phosphorylated peptides during electron-transfer dissociation tandem mass spectrometry. Anal. Chem. **87**, 6990–6994 (2015)
43. Salek, M., Alonso, A., Pipkorn, R., Lehmann, W.D.: Analysis of protein tyrosine phosphorylation by nanoelectrospray ionization high-resolution tandem mass spectrometry and tyrosine-targeted product ion scanning. Anal. Chem. **75**, 2724–2729 (2003)
44. Steen, H., Pandey, A., Andersen, J.S., Mann, M.: Analysis of tyrosine phosphorylation sites in signaling molecules by a phosphotyrosine-specific immonium ion scanning method. Sci. STKE. **2002**, pl16 (2002)
45. Perez-Riverol, Y., Csordas, A., Bai, J., Bernal-Llinares, M., Hewapathirana, S., Kundu, D.J., Inuganti, A., Griss, J., Mayer, G., Eisenacher, M., Perez, E., Uszkoreit, J., Pfeuffer, J., Sachsenberg, T., Yilmaz, S., Tiwary, S., Cox, J., Audain, E., Walzer, M., Jarnuczak, A.F., Ternent, T., Brazma, A., Vizcaino, J.A.: The PRIDE database and related tools and resources in 2019: improving support for quantification data. Nucleic Acids Res. **47**, D442–d450 (2019)